Journal of Physics: Theories and Applications E-ISSN: 2549-7324 / P-ISSN: 2549-7316
J. Phys.: Theor. Appl. Vol. 7 No. 2 (2023) 152-167 doi: 10.20961/jphystheor-appl.v7i2.78375

Shielding parameters of leaded cement mortar

Yassin A. Abdel-Razek

Nuclear Materials Authority, El Maadi, El Qattamiya Road, P.O. Box 530 El Maadi, Cairo.

Email: ya_sien@hotmail.com

Received 29 August 2023, Revised 18 September 2023, Published 30 September 2023

Abstract: The Cathode ray tubes (CRTs) represent more than 70% of global e-waste sets. The glass of the CRT is doped with lead to prevent emission of radiations especially electrons. The glass at the panel and neck of the CRT along with the cement mortar, a mixture of 70% neck glass and 30% cement (mix70), are investigated mathematically as shielding materials from photons having energies in the range 0.06-3 (MeV). Experimentally the material mix70 is tested at energies 0.238 and 0.583 (MeV). Good agreement was recognized between the calculated shielding parameters and that obtained experimentally while complete equality between the calculated parameters carried out using the online XCom software or Phy-X software except at low energies for concrete material. Glass from panel, neck and mix70 have acceptable shielding characteristics at and below the energy 0.238 (MeV) or generally at the X-ray region. Neck glass has good shielding parameters at the chosen energy region and it is nominated as a shielding material for many nuclear applications. To enhance the shielding characteristics of the material mix70 it should be compacted during preparation to get higher density. Then we make the comparison between three concentrations (90%, 80%, 70%) of (CRT) funnel glass based on shielding efficiency. the good results done with mix 70%. The present work tested the shielding properties of leaded glass composites to find out its integrity for practical shielding applications and radiological safety.

Keyword : CRT Recycle, E-waste, Cement mortar, Leaded glass, shielding, attenuation coefficient, XCom, Phy-X

1. Introduction

The disposal of waste electric and electronic equipment (WEEE), especially the cathode ray tubes (CRTs) used in computer and television monitors becoming a global environmental issue that must be eliminated urgently [1,2]. A large number of cathode ray tubes (CRTs), which account for over 70% of global e-waste sets [3,4], are eliminated each year as a result of update and replacement of display products It has been generated in a short time and has just begun to be managed [5,6]. Based on the United Nations University (UNU) statistics, the global generation of e-waste was around 41.8 Mt, the waste CRTs accounted for about 6.3 Mt in 2014, to which Asia contributed 2.5 Mt, and the global e-waste production is expected to increase up to 50 Mt after three years [7]. It is estimated that CRT occupies around 65% mass of a television or computer monitor and is constituted of 85% glass, in which a front panel

for screen contributes 65%, a back neck for enveloping the electron gun, 5%, and a funnel for connecting the panel and the neck, 30% [1,8]. The CRT glass can be divided into low lead glass and high lead glass according to its lead oxide content, the panel containing 0–3 wt.% lead oxide belongs to the former type, while the funnel and neck for shielding harmful radiation respectively containing 22−25 wt.% and ~30 wt.% lead oxide [2,9]. Dumped CRTs are moved to be incinerated and discarded in landfills as municipal solid waste [10,11]. Heavy metals such as lead and zinc have significant toxic effects and risks on most biological organisms (including human beings) and ecological environments [12,13], and the pollution of heavy metals poses great threat to the environment and human beings due to its characteristics of persistence, non-degradability and bioaccumulation [14]. the eco-efficient management of CRT waste has become a priority of global concern in order to suitably and safely eliminate such waste [15]. So, the waste CRT is classified as hazardous waste in European Waste Catalogue 2002 and China National Hazardous Waste List 2016 since it contains 22%−28% highly toxic metal lead as well as other high metals such as barium and strontium [16]. One possibility to reducing CRT waste is recycling into a raw material for the production of concrete. There has been extensive research regarding the feasibility of this approach [17,18]. Use as a concrete-based shield for application in medical radiation, industry and nuclear power plants has been studied [19-22]. Unsuitable disposal of CRT waste glass will pose a considerable threat to the environment as well as humanity [2,23]. Generally, closed-loop and open-loop recycling process systems are adopted in the recycling of CRTs [23,24].The closed-loop process system refers to the recycling of CRTs by sending waste CRTs to CRT factories to obtain lead and lead-free glasses required for manufacturing new CRTs in the manufacturing chain itself [25,26] . The open-loop process system mainly involves the recycling and utilization of CRT glass in the manufacture of new products. Recycled CRT glass is another source for fabricating new glass material as radiation shielding because of its unique properties including transparency, high strength and excellent corrosion resistance. Also, changes in the composition and preparation processes can alter the glass properties. Hence, it has many possible uses in the nuclear radiation field and has also been examined as a potential engineering material to replace concrete [27]. The existing technology of recovering lead from waste CRT glass is not sophisticated, which has disadvantages such as high energy consumption, low recovery efficiency and possible environmental pollution [28,29]. The disposal of waste CRT glass is becoming an urgent problem to be solved [30]. Incidentally, the addition of BaO into recycled glass not only optimizes its radiation shielding property, but also reduces the environmental toxicity of Pb by replacing some Pb atoms with Ba atoms. Barium is less naturally occurring in silicate systems than lighter alkaline earths such as Mg, Ca, and Sr. Higher mass for thermal resistance, and radiation resistance with higher electron density of the glass system have been received by the addition of higher atomic number Ba atoms. Consequently, barium silicate components have received a great deal of attention for heat and radiation shielding applications [31,32]. As mentioned above, the CRT-based glass system has been selected to assess the possibility of using the system

as a new radiation shielding material. Without considering its toxic components, alternative applications for secondary CRT glass have been processed to bricks, decorative tile, nuclear waste encapsulation, construction aggregates, fluxing agent, and sandblasting medium [33-35]. However, it is estimated that only about 26% of the discarded CRTs are recycled while the remaining 59% are landfilled due to the lack of satisfied recycling approaches globally [36]. Meanwhile, concrete material has been widely used in construction, and the aggregate accounts for 60%−75% of the volume of concrete. Due to huge demand for fine aggregate, the natural river sand in China has nearly been exhausted [37] , so, CRT funnel glass has been studied as a replacement for natural sand as fine aggregate in mortar or concrete by many researchers [30,36,38,39].

2. Experimental Methods

2.1. Measurement of the γ-spectrum of natural thorium

A calibration source containing natural thorium of small activity is used for the study. The source is capsulated in a plastic disc shaped envelope. A portable identifier PM 1704 multichannel analyzer containing CsI (Tl) detector with 1023 channels was used to record the γ-spectrum of the thorium source. The PM 1704 instrument is self-calibrated for channel/energy conversion [40]. The spectrum of thorium through air is recorded and then one-by-one plate of the leaded cement mortar or mix70 is added successively between the source and the identifier and the spectrum is recorded each time. Each measurement is carried out for one hour while these measurements were achieved in the open air, Fig. 1. The spectra of natural thorium are saved in the PM 1704 device as data files which were transferred to the PC via USB connection.

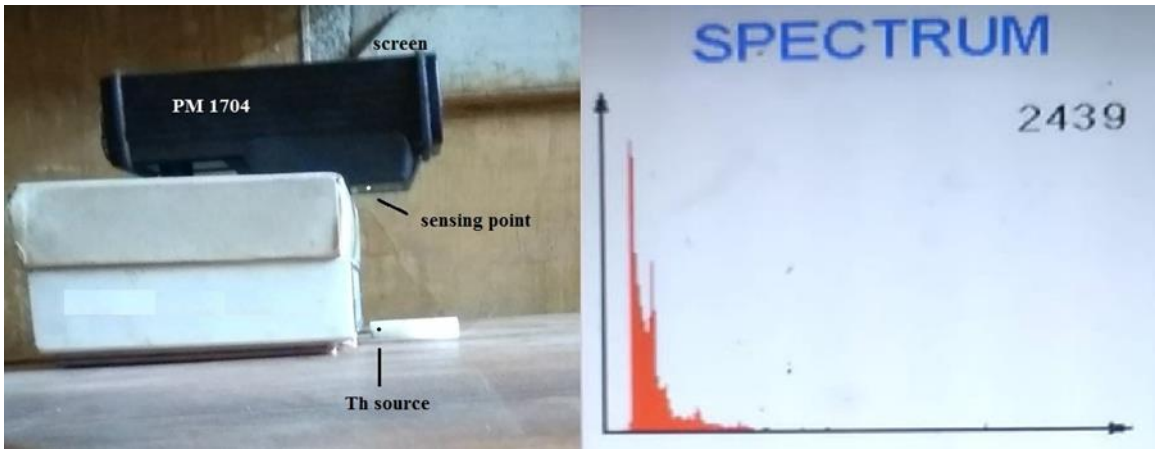

Figure 1. Measurement set-up. The PM 1704 identifier is fixed with its sensing point adjacent vertically the Th-source at a suitable distance (left).The spectrum of Th is displayed on the PM 1704 screen and the time elapsed for the measurement in seconds is illustrated (right).

2.2. Determination of the signal intensity I

Natural thorium emits more than 50 X and γ-rays with energies below 1000 (keV) from its decay chain [41]. PM 1704 identifies natural thorium only by 7 energies

(signals) [40]. This study chose the two narrow, intense and easy-to-separate signals at E1 (238keV, Pb-212) and E3 (583keV, Tl-208).

To determine the characteristics of each signal, ORIGIN5® software was used. The signals at E1 and E3 for each measurement were fitted as Gaussian signals. This enables excluding the noise and background of each measurement and obtains the accurate values of the intensity I and the width (ΔE) of the signal.

Spectra of the natural thorium through air and through the different thicknesses of the mixture mix70 (leaded concrete) are shown in Fig. 2.

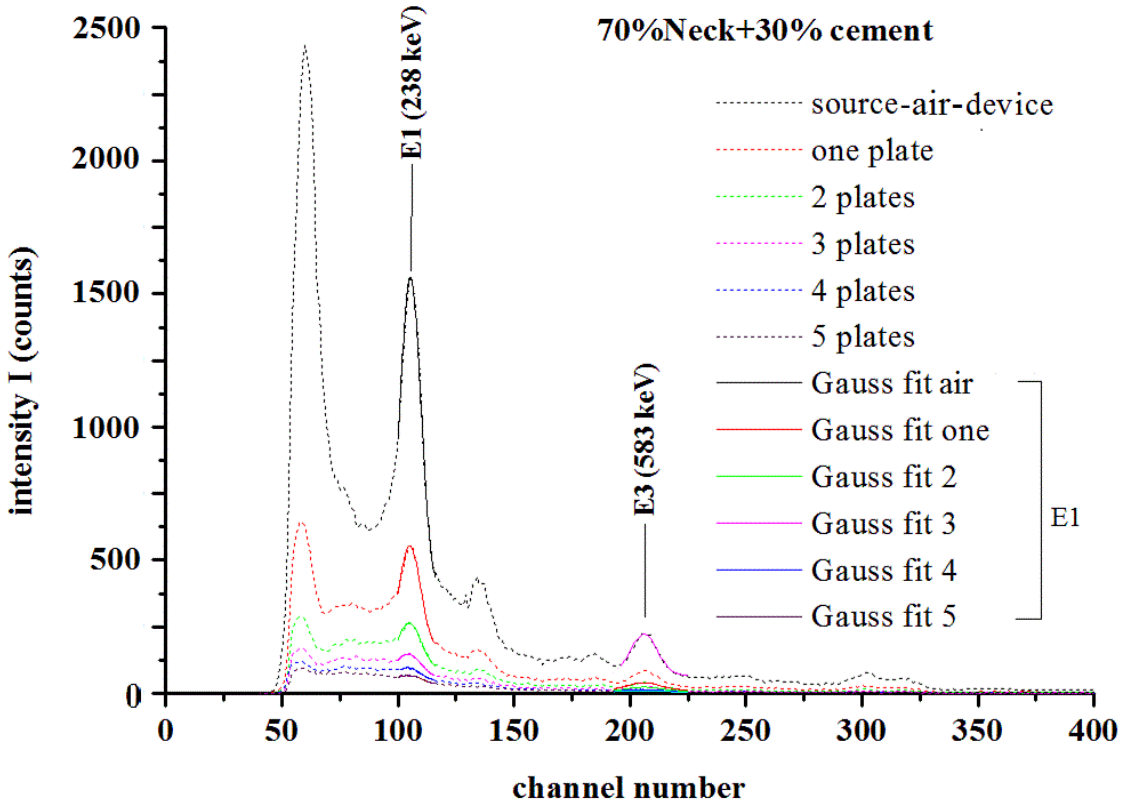

Figure 2. Gamma spectrum of the natural thorium through air and through different numbers of 1.1 cm plates constructed from the mixture of 70% neck powder glass and 30% cement (leaded concrete). Gauss fit of the signals at E1 and E3 is illustrated.

2.3. Calculation of the shielding parameters of CRT glass at the panel and the neck

Two online softwares were employed to calculate the shielding parameters of the studied glasses; Phy-X [42] and XCom [43]. The calculated parameters are the mass attenuation coefficient μ/ρ (cm^2/g), the linear attenuation coefficient μ (cm^{-1}) and the half value layer HVL (cm). Along with the parameters of the CRT glass from the panel and neck, the parameters of the mixture mix70 and concrete NBS were calculated for comparison. The data about the fraction by weight of the oxides composing each material are fed to both software and the results of the chosen parameters are saved as EXCEL files which then fed to ORIGIN5® software to plot these data. The mentioned

EXCEL files contain also the calculated elemental composition of the studied materials as fractions by weights.

3. Results and Discussions

3.1. Elemental composition of the studied materials

Table 1. Elemental composition of five specimens (fraction by weight) as calculated by XCom.

Z		Panel	Neck	Cement OPC	Concrete NBS	Mix70
1	H				0.0056	
8	O	0.392829	0.376715	0.354657	0.4983	0.367301
11	Na	0.040479	0.033352	0.000483	0.0171	0.019324
12	Mg	0.001651	0.007105	0.004057	0.0024	0.005804
13	Al	0.015351	0.017608	0.026918	0.0456	0.021582
14	Si	0.272734	0.259314	0.10258	0.3158	0.192421
15	P	0.000266	0.000165			0.000094
16	S	0.000731	0.000491	0.005649	0.0012	0.002692
17	Cl	0.000507	0.000566			0.000324
19	K	0.070891	0.069166	0.00054	0.0192	0.039877
20	Ca	0.01022	0.023441	0.479246	0.0826	0.217975
22	Ti	0.002979	0.001412			0.000810
26	Fe	0.00078	0.001384	0.025869		0.011834
29	Cu	0.000162	0.001280			0.000734
30	Zn	0.00220	0.001287			0.000738
38	Sr	0.075212	0.020881			0.011969
40	Zr	0.014116	0.004535			0.002600
51	Sb	0.003219	0.002126			0.001218
56	Ba	0.083570	0.026760			0.015339
58	Ce	0.002312	0.013120			0.007521
82	Pb	0.009792	0.139291			0.079843

Attenuation of X and γ radiations through any material is a result of interaction of the incident photons with the orbital electrons of the elements composing this material by one of three processes; photoelectric effect in which a photon with enough energy delivers its energy to an electron to leave the orbit, Compton scattering when the photon has higher energy such that only a part of its energy rejects an electron out of its orbit and the photon moves in a different direction with the rest energy or pair production which occurs at the field of the nucleus when the photon of energy higher than 1.02 (MeV) splits to a positron and an electron. Accordingly, the attenuation of the photons traversing in a material is dependent on the number of electrons or the atomic number Z of this material. Table 1 represents the elemental composition of the materials panel

glass, neck glass, cement OPC, concrete NBS [44] and the mixture mix70 as fractions by weights.

3.2. Calculation of the mass attenuation coefficient μ/ρ

The total mass attenuation coefficient or the mass attenuation coefficient μ/ρ of a material is the sum of the mass attenuation coefficients of the processes photoelectric, Compton scattering and pair production of this material. Fig. (3) compares the calculated values of μ/ρ of four materials for photons having energies in the interval 0.06-3 (MeV) which covers the most frequent sources used for various applications. Concrete NBS has the lower values of μ/ρ since it contains the elements of low values of ($Z \leq 20$). Elements having higher atomic numbers uplifted the values of μ/ρ. Thirteen percent of these elements raised the value three times for the mixture mix70 while the values of μ/ρ are raised almost five times with concentrations 19% and 21% of elements of ($Z > 20$) for pure panel and neck glasses, respectively.

The K-absorption edge (K-edge) refers to the abrupt increase in the photoelectric absorption of x-ray photons observed at an energy level just beyond the binding energy of the k-shell electrons of the absorbing atom [45]. The K-edge of lead (Pb) appears at 82 (keV) as shown in Fig. 3. Values of the mass attenuation coefficient μ/ρ for photons with energies beyond the K-edge are arranged according to the concentration of lead in the materials of pure glasses of panel and neck and the mixture mix70. In the energy range 0.7-3 (MeV) the values of μ/ρ are apparently independent on the chemical composition and are equal for the four studied materials.

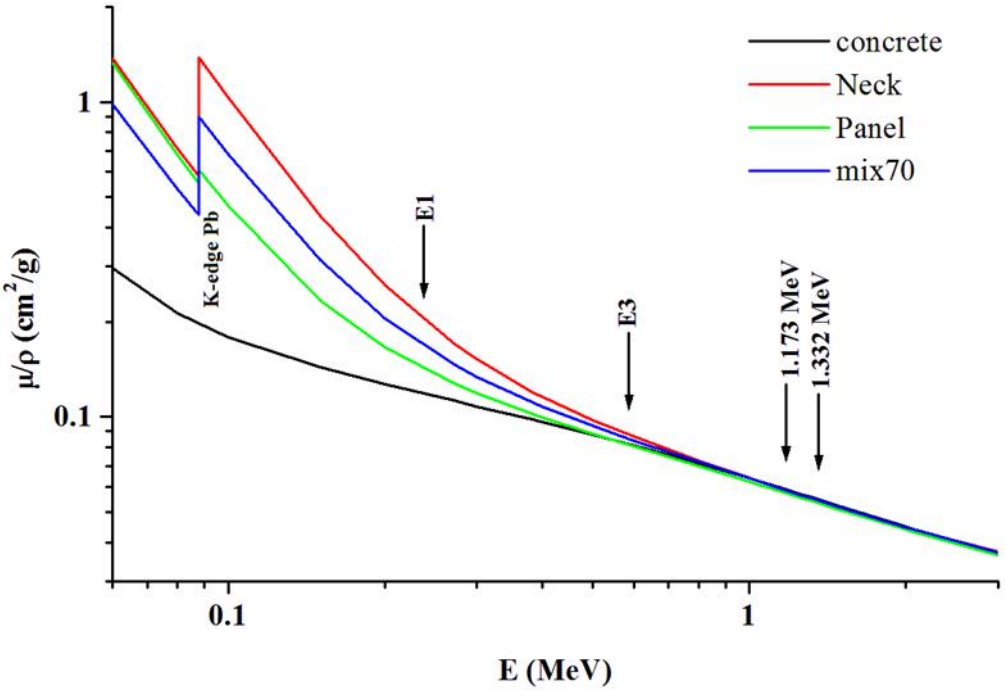

Figure 3. Total mass attenuation coefficients μ/ρ (cm^2/g) calculated by XCom for the four chosen materials over the energy range 0.06-3 (MeV).

In comparison between the results obtained by Phy-X and XCom softwares, Fig. 4 shows the calculated values of the mass attenuation coefficient μ/ρ for the four studied materials.

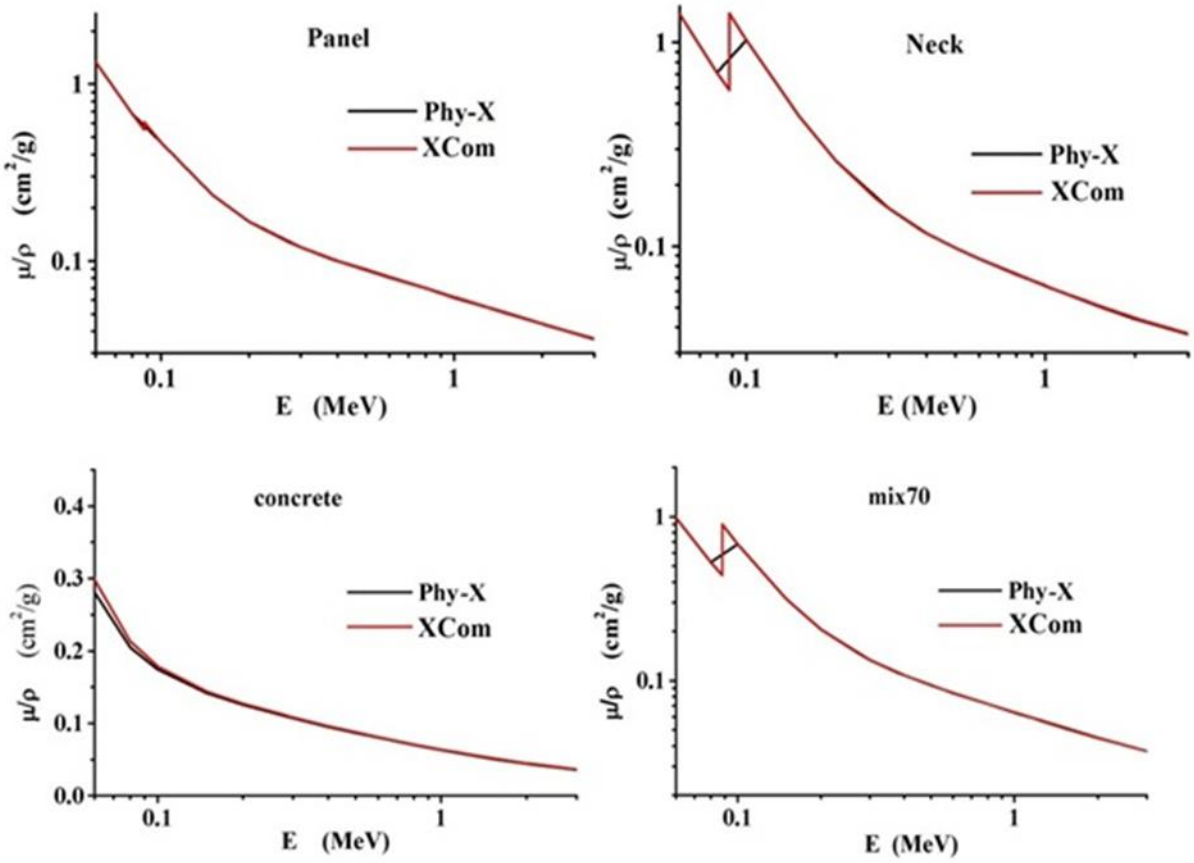

Figure 4. Mass attenuation coefficient μ/ρ (cm2/g) as calculated by the online softwares Phy-X and XCom for the studied materials over the energy range 0.06-3 (MeV).

Slight differences between the values of μ/ρ obtained by the two softwares for concrete NBS at energies below 0.1 (MeV) while complete equality between them appears at energies in the range 0.1-3 (Mev). The values of μ/ρ for the other materials panel and neck glasses and mix70 show complete equality when calculated by Phy-X or XCom except at the K-edge of lead. This is because the default table of energy embedded in Phy-X has little energy values at the K-edge while that of XCom has more energy values. However, the chosen energies at E1 and E3 are far beyond the mentioned differences. Table (2) represents the calculated values of the mass attenuation coefficient μ/ρ for the four studied materials at the chosen energies E1 and E3 along with the two characteristic energies of ^{60}Co at 1.173 and 1.333 (MeV). The values of μ/ρ for the glasses of panel, neck and mix70 are higher than that of concrete NBS at photon energy 0.238 (MeV). Obviously, at the higher energies the values of μ/ρ are in the same vicinity for the different materials.

Table 2. Total mass attenuation coefficients μ/ρ (cm2/g) calculated by XCom for the four chosen materials at four different energies E (MeV).

E (MeV)	Panel	Neck	Concrete NBS	mix70
0.238	0.142	0.203	0.118	0.168
0.583	0.082	0.088	0.082	0.086
1.173	0.057	0.059	0.059	0.059
1.333	0.054	0.055	0.053	0.055

3.3. Determination of the linear attenuation coefficient μ of the cement mortar

If a beam of X or γ photons having intensity I_0 is passing through a material it suffers attenuation along its passage due to the interaction with the electrons of the elements composing this material. The decrease in the intensity is dependent not only on the atomic number of the material but also on the electron density or the density of the material. Here the linear attenuation coefficient μ is more informative about the shielding potential of the studied material. The linear attenuation coefficient is defined as the number of interactions carried out along one centimeter inside the material, (cm^{-1}). μ has a simple relation with μ/ρ via the density of the material ρ.

The attenuation of a beam of intensity I0 through a material is described by the equation [45]:

$$I=I0*\exp(-\mu x) \quad (1)$$

or

$$\ln(I0/I)=\mu x \quad (2)$$

where

I_0 is the initial beam intensity,

I is the intensity of the beam at depth or thickness x (cm) inside the material,

μ is the linear attenuation coefficient of the material (cm^{-1}).

Fig. 5 shows the attenuation of the number of photons having energies E1 and E3 with the thickness of the cement mortar, mix70 (left). Also, Fig (5) represents the linear relationship between both sides of Eqn. (2), (right). The slopes of the two straight lines equal the attenuation coefficients of mix70 at E1 and E3 which have the values of 0.326±0.006 and 0.176±0.006 (cm^{-1}) respectively. Table (3) represents the calculated and experimental values of μ for the material mix70.

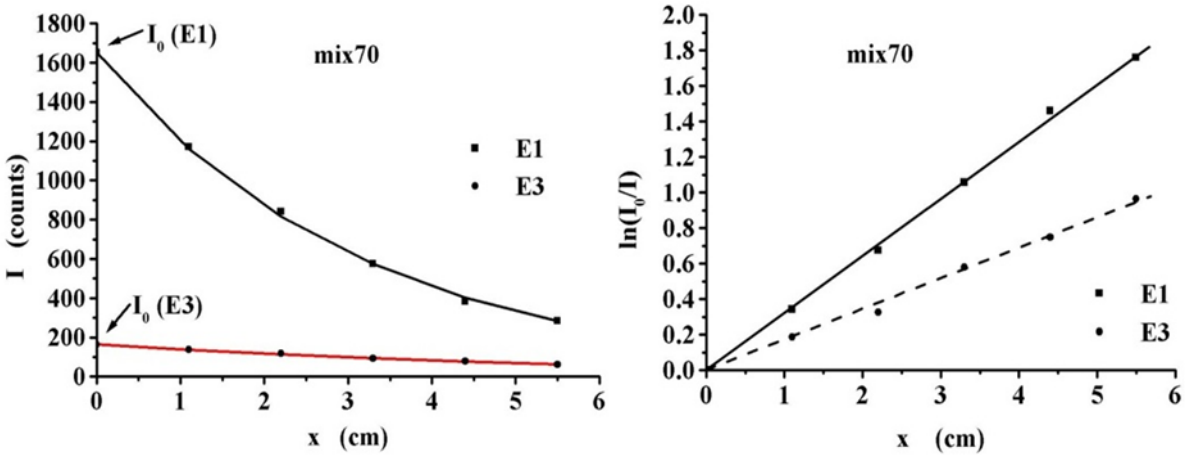

Figure 5. Typical attenuation of the intensity I of the signals at E1 and E3 with the thickness x of the leaded concrete, (left). Regression of $\ln(I_0/I)$ over x, (right). The slope of the straight line equals the value of the linear attenuation coefficient μ (cm^{-1}) for the studied material at the desired energy.

Table 3. Calculated and experimental values of μ (cm^{-1}) of the material mix70.

Energy (MeV)	μ (cm-1)		Error%
	calculated	experimental	
0.238	0.311	0.326±0.006	6.4
0.583	0.159	0.176±0.006	13

The experimental value of the linear attenuation coefficient μ estimated for mix70 material appears in good agreement with the calculated value either by Phy-X software or XCom software. However, the respective high error in estimating μ at the energy 0.583 (MeV) may be due to the low counts of photons at this energy which increase the statistical errors.

Density ρ of the materials of mix70 and the bulk neck glass was measured using Archimedes' method to have the values of 1.85± 0.05 and 3.1±0.2 (g/cm^3), respectively.

Abdel-Razek calculated the shielding parameters of heavy natural minerals; rutile, ilmenite and magnetite using XCom software. He recognized that the apparent similarity in chemical composition and close densities of the studied minerals resulted in close values of the shielding parameters of them [46]. Hager et al. studied the shielding characteristics of natural bentonite [47]. They found that compressing bentonite under a pressure of 150 (bar) raised the density of its material by 35%. This increase in density enhanced the value of the linear attenuation coefficient μ by more than 50%. So, they concluded that compressing a material increases the electron density inside the material and enhance its shielding characteristics.

Optical and shielding properties of CRT manufactured by Hitachi (after year 2000) were studied [48]. Many other researchers prepared different materials of glass with different values of density [49-52]. Table 4 represents the chemical composition of the different glasses and bentonite. Fig (6) represents the variation of the calculated values of the attenuation coefficient μ with the photon energy in different glasses and in

bentonite over the energy range 0.06-3 (MeV). The density of a material is presented at the right of its line. The figure clarifies that the values of μ for the studied materials are arranged according to the values of their densities. One exception is recognized for the material mix70 which has a lower density than concrete while it has higher values of μ at energies below 0.32 (MeV). Again, this is due to the elements of atomic number higher than 21 and due to the K-edge of lead which enhances the shielding characteristics at energies around it.

In the scope of all the above remarks, the material of mix70 should be compressed during preparation in order to enhance its shielding characteristics.

Table 4. Code, chemical composition and density ρ of different glasses and bentonite.

Code	Chemical composition	ρ (g/cm3)	Ref.
Bentonite	Fraction by weight 0.3SiO2+0.135Al2O3+0.0034P2O5+0.0034 TiO2+0.032FeO3+0.152CaO+0.0403MgO+ 0.014Na2O+0.0061K2O+0.3034 water&organics	Natural, 0.85	
Mix70	Elemental, Table (1), this study	Pressed, 1.12	[47]
Concrete	Elemental, Table (1)		
Neck	Elemental, Table (1), this study	1.85	
Neck2	Fraction by weight	2.25	[44]
B1	%mol, 80B2O3+20PbO	3.1	
A4	%mol, 35PbO+10TeO2+10MgO+10Na2O+35B2O 3	3.25	[48]
Te20BPb-5	%mol, 60TeO2+20B2O3+20PbO	3.342	[50]
Ge5	%mol, 60GeO2+40PbO	3.923	[52]

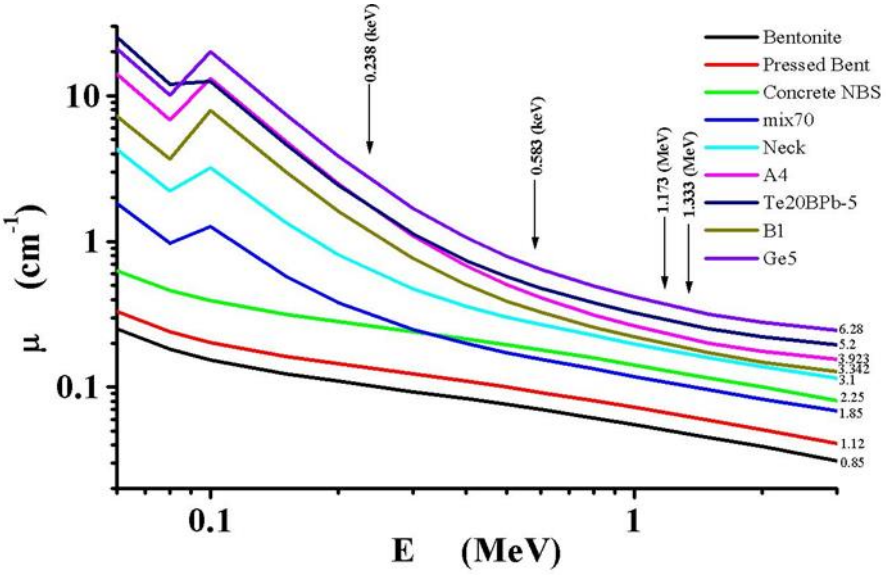

Figure 6. The variation of the attenuation coefficient μ with photon energy E in some materials of different densities.

3.4. Calculation of the half value layer HVL of the studied materials

The half value layer HVL of a material is the thickness of that material which reduces the initial intensity to one half of its value. This is calculated as follows:

$$HVL=\ln(2)/\mu \quad (3)$$

HVL is calculated in (cm). Table 5 represents the linear attenuation coefficient μ and the half value layer HVL calculated for some materials.

Concerning density, concrete NBS has a moderate one and accordingly it has moderate shielding characteristics. Lighter materials have poorer characteristics which necessitate thicker shields for a desired energy. This may contradict the economics of a shielding project. The material mix70 has better characteristics than concrete at and below the energy 0.238 (MeV) or generally at the X-ray region. However, concrete restores its position as a heavier material at the higher energies. The glass from the neck of the CRT has good shielding parameters at all the chosen energies which nominate this material as a shielding material for many nuclear applications.

4. Conclusions

The glass of the CRT is doped with lead to prevent emission of radiations especially electrons. The glasses at the panel and neck of the CRT along with a mixture of 70% neck glass and 30% cement (mix70) are investigated mathematically as shielding materials from photons having energies in the range 0.06-3 (MeV). Experimentally the material mix70 is tested at energies 0.238 and 0.583 (MeV). Good agreement was recognized between the calculated shielding parameters and that obtained experimentally while complete equality between the calculated parameters carried out using the online XCom software or Phy-X software except at low energies for concrete material. Glass from panel, neck and mix70 have acceptable shielding characteristics at

and below the energy 0.32 (MeV) or generally at the X-ray region. Neck glass has good shielding parameters at the chosen energy region and it is nominated as a shielding material for many nuclear applications. To enhance the shielding characteristics of the material mix70 it should be compacted during preparation to get higher density.

Table 5. Linear attenuation coefficient μ and half value layer HVL for glasses and bentonite at the chosen energies.

Code	E (MeV)	0.238	0.583	1.173	1.333
Pressed bentonite	μ (cm-1)	0.136	0.094	0.068	0.064
	HVL (cm)	5.09	7.35	10.22	10.91
Mix70	μ (cm-1)	0.311	0.159	0.109	0.102
	HVL (cm)	2.23	4.36	6.35	6.81
Concrete	μ (cm-1)	0.266	0.185	0.133	0.119
	HVL (cm)	2.61	3.76	5.22	5.81
Neck	μ (cm-1)	0.629	0.273	0.183	0.171
	HVL (cm)	1.10	2.54	3.79	4.07
Neck2	μ (cm-1)	0.947	0.313	0.193	0.179
	HVL (cm)	0.73	2.21	3.60	3.88
Ge5	μ (cm-1)	2.651	0.666	0.368	0.339
	HVL (cm)	0.26	1.04	1.88	2.04

References

[1] Andreola, F., Barbieri, L., Corradi, A., Lancellotti, I., 2007. CRT glass state of the art a case study: recycling in ceramic glazes. J. Eur. Ceram. Soc. 27, 1623–1629. https://doi.org/10.1016/j.jeurceramsoc.2006.05.009.

[2] Nnorom, I.C., Osibanjo, O., Ogwuegbu, M.O.C., 2011. Global disposal strategies for waste cathode ray tubes. Resour. Resour. Conserv. Recy. 55 (3), 275–290. https://doi.org/10.1016/j.resconrec.2010.10.007.

[3] Gable C, Sirman B. Computer and electronics product stewardship: Are we ready for the challenge [J]. Environmental Quality Management, 2010, 11(1): 35−45.

[4] Mueller J R, Boehm M W, Drummond C. Direction of CRT waste glass processing: Electronics recycling industry communication [J]. Waste Management, 2012, 32(8): 1560−1565.

[5] Xing, M., Wang, J., Fu, Z., Zhang, D., Wang, Y., Zhang, Z., 2018. Extraction of heavy metal (Ba, Sr) and high silica glass powder synthesis from waste CRT panel glasses by phase separation. J. Hazard. Mater. 347, 8–14. https://doi.org/10.1016/j.jhazmat.2017.12.046.

[6] Xu, Q., Li, G., He, W., Huang, J., Shi, X., 2012. Cathode ray tube (CRT) recycling: current capabilities in China and research progress. Waste Manag. 32, 1566–1574. https://doi.org/10.1016/j.wasman.2012.03.009.

[7] Balde C, Wang F, Kuehr R, Huisman J. The global e-waste monitor–2014 [R]. Bonn: United Nations University, 2015.

[8] Mear F, Yot P, Cambon M, Ribes M. The characterization of waste cathode-ray tube glass [J]. Waste Management, 2005, 26(12): 1468−1476.

[9] Ling Tung-chai, Poon Chi-sun, Lam Wai-shung, CHAN Tai-po, FUNG K K. Utilization of recycled cathode ray tubes glass in cement mortar for X-ray radiation-shielding applications [J]. Journal of Hazardous Materials, 2011, 199(2): 321−327.

[10] Gong, Y., Tian, X.M., Wu, Y.F., Tan, Z., Lv, L., 2016. Recent development of recycling lead from scrap CRTs: a technological review. Waste Manag. 57, 176–186. https://doi.org/10.1016/j.wasman.2015.09.004.

[11] Yamashita, M., Wannagon, A., Matsumoto, S., Akai, T., Sugita, H., Imoto, Y., Komai, T.,Sakanakura, H., 2010. Leaching behavior of CRT funnel glass. J. Hazard. Mater. 184, 58–64. https://doi.org/10.1016/j.jhazmat.2010.08.002.

[12] Feng Ning-chuan, Guo Xue-yi. Characterization of adsorptive capacity and mechanisms on adsorption of copper, lead and zinc by modified orange peel [J]. Transactions of Nonferrous Metals Society of China, 2012, 22(5): 1224−1231.

[13] Song Jie, Guo Zhao-hui, Xiao Xi-yuan, Miao Xu-feng, Wang Feng-yong. Environmental availability and profile characteristics of arsenic, cadmium, lead and zinc in metal-contaminated vegetable soils [J]. Transactions of Nonferrous Metals Society of China, 2009, 19(3): 765−772.

[14] Jiang Bo-feng, Sun Wei-ling. Assessment of heavy metal pollution in sediments from Xiangjiang River (China) using sequential extraction and lead isotope analysis [J]. Journal of Central South University, 2014, 21(6): 2349−2358.

[15] Hu, B., Hui, W., 2018. Lead recovery from waste CRT funnel glass by high-temperature melting process. J. Hazard. Mater. 343, 220–226. https://doi.org/10.1016/j.jhazmat.2017.09.034

[16] LV Jian-fang, YANG Hong-ying, JIN Zhe-nan, MA Zhi-yuan, SONG Yan. Feasibility of lead extraction from waste cathode-ray-tubes (CRT) funnel glass through a lead smelting process [J]. Waste Management, 2016, 57: 198−206.

[17] Walczak, P., Małolepszy, J., Reben, M., Rzepa, K., 2015. Mechanical properties of concrete mortar based on mixture of CRT glass cullet and fluidized fly ash. ProcediaEng. 108, 453–458. https://doi.org/10.1016/j.proeng.2015.06.170.

[18] Zhao, H., Poon, C.S., Ling, T.C., 2013. Utilizing recycled cathode ray tube funnel glass sand as river sand replacement in the high-density concrete. J. Clean. Prod. 51,184–190. https://doi.org/10.1016/j.jclepro.2013.01.025.

[19] Akkurt, I., Akyıldırım, H., Mavi, B., Kilincarslan, S., Basyigit, C., 2010. Radiation shielding of concrete containing zeolite. Radiat. Meas. 45, 827–830. https://doi.org/10.1016/j.radmeas.2010.04.012.

[20] Ling, T.C., Poon, C.S., Lam, W.S., Chan, T.P., Fung, K.K.. Utilization of recycled cathode ray tubes glass in cement mortar for X-ray radiation-shielding applications. J Hazard Mater. 2012 Jan 15;199-200:321-7. doi: 10.1016/j.jhazmat.2011.11.019. Epub 2011 Nov 10. PMID: 22118845.

[21] Meng, Y., Ling, T.C., Mo, K.H., 2018. Recycling of wastes for value-added applications in concrete blocks: an overview. Resour. Conserv. Recycl. 138,

298–312. https://doi.org/10.1016/j.resconrec.2018.07.029.

[22] Waly, E.S.A., Fusco, M.A., Bourham, M.A., 2017. Impact of specialty glass and concrete on gamma shielding in multi-layered PWR dry casks. Prog. Nucl. Energy 94, 64–70. https://doi.org/10.1016/j.pnucene.2016.09.017.

[23] Jang Y C, Townsend T G. Leaching of lead from computer printed wire boards and cathode ray tubes by municipal solid waste landfill leachates [J]. Environmental Science & Technology, 2003, 37(20): 4778−4784.

[24] XU Qing-bo, LI Guang-ming, HE Wen-zhi, HUANG Ju-wen, SHI Xiang. Cathode ray tube (CRT) recycling: Current capabilities in China and research progress [J]. Waste Management, 2012, 32(8): 1566−1574.

[25] Mostaghel S, Samuelsson C. Metallurgical use of glass fractions from waste electric and electronic equipment (WEEE) [J]. Waste Manag, 2009, 30(1): 140−144.

[26] Andreola F, Barbieri L, Corradi A, Ferrari A M, Lancellotti, Neri P. Recycling of EOL CRT glass into ceramic glaze formulations and its environmental impact by LCA approach [M]. International Journal of Life Cycle Assessment, 2007, 12(6): 448−454.

[27] Laopaiboon, R., Bootjomchai, C., Chanphet, M., Laopaiboon, J., 2011. Elastic properties investigation of gamma-radiated barium lead borosilicate glasses using ultrasonic technique. Ann. Nucl. Energy 38, 2333–2337. https://doi.org/10.1016/j.anucene.2011.07.035.

[28] Gong Yu, Tian Xiang-miao, Wu Yu-feng, Tan Zhe, LV Lei. Recent development of recycling lead from scrap CRTs: A technological review [J]. Waste Management, 2016, 57: 176−186.

[29] Okada T, Yonezawa S. Energy-efficient modification of reduction-melting for lead recovery from cathode ray tube funnel glass[J]. Waste Management, 2013, 33(8): 1758−1763.

[30] Yuan Wen-yi, Li Jin-hui, Zhang Qi-wu, Saito F, Yang Bo. Lead recovery from cathode ray tube funnel glass with mechanical activation [J]. Journal of the Air & Waste Management Association, 2013, 63(1): 2−10.

[31] Lara, C., Pascual, M.J., Duran, A., 2004. Glass-forming ability, sinterability and thermal properties in the systems RO–BaO–SiO2 (R ¼ Mg, Zn). J. Non-Cryst. Solids 348,149–155. https://doi.org/10.1016/j.jnoncrysol.2004.08.140

[32] Rai, M., Mountjoy, G., 2014. Molecular dynamics modelling of the structure of barium silicate glasses BaO-SiO2. J. Non-Cryst. Solids 401, 159–163. https://doi.org/10.1016/j.jnoncrysol.2013.12.026.

[33] Hreglch S, Falcone R, Vallotto M. The recycling of end-of-life panel glass from TV sets in glass fibres and ceramic productions [M]. London: Thomas Telford Publishing, 2001.

[34] Gregory J R, Nadeau M C, Kirchain R E. Evaluating the economic viability of a material recovery system: The case of cathode ray tube glass [J]. Environmental Science & Technology, 2009, 43(24): 9245−9251.

[35] Ling Tung-chai, Poon Chi-sun. Use of recycled CRT funnel glass as fine

aggregate in dry-mixed concrete paving blocks [J]. Journal of Cleaner Production, 2014, 68(2): 209−215.

[36] Rachad A M. Recycled waste glass as fine aggregate replacement in cementitious materials based on Portland cement [J]. Construction & Building Materials, 2014, 72: 340−357.

[37] Liu Tie-jun, Song Wen, Zou Du-jian, Li Lei. Dynamic mechanical analysis of cement mortar prepared with recycled cathode ray tube (CRT) glass as fine aggregate [J]. Journal of Cleaner Production, 2018, 174: 1436−1443.

[38] Sikora P, Horszczaruk E, Rucinsca T. The effect of nanosilica and titanium dioxide on the mechanical and self-cleaning properties of waste−glass cement mortar [J]. Procedia Engineering, 2015, 108: 146−153.

[39] Yao Zhi-tong, Ling Tung-chai, Sarker P K, Su Wei-ping, Liu Jie, Wu Wei-hong, Tang Jun-hong. Recycling difficult-to-treat e-waste cathode-ray-tube glass as construction and building materials: A critical review [J]. Renewable & Sustainable Energy Reviews, 2017, 81: 595−604.

[40] Polimaster (2011). PM 1704 Built-In Software Guide, First edition, July 2011, Russia.

[41] Sadasivan, S. and Raghunath, V. M. (1982). Intensities of Gamma Rays in the 232Th Decay Chain. Nuclear Instruments and Methods 196, 561-563. Letter to the editor.

[42] Şakar, Erdem, Özpolat,Özgür Fırat, Alım, Bünyamin, Sayyed, M.I., Kurudirek, Murat (2020). Phy-X / PSD: Development of a user friendly online software for calculation of parameters relevant to radiation shielding and dosimetry. Radiation Physics and Chemistry. 166, 108496.

[43] Berger, M.J., Hubbell, J.H. (1999) XCOM: Photon Cross Sections Data Base, Web version, 1.2. National Institute of Standards and Technology, Gaithersburg (1999) (Originally published as NBSIR 87-3597 “XCOM: Photon cross sections on a personal computer”). https://physics.nist.gov/PhysRefData/Xcom/html/xcom1.html

[44] Mann, Kulwinder Singh, Rani, Asha, Heer, Manmohan Singh (2015). Shielding behaviors of some polymer and plastic materials for gamma-rays. Radiation Physics and Chemistry, 106, 247-254.

[45] Knoll, G.F. (2000): Radiation Detection and Measurement. 3rd edition. John Wiley & Sons, Inc. 802p.

[46] Abdel-Razek, Yassin A. (2019): Calculation of the Shielding Parameters of Some Natural Minerals. J. Rad. Nucl. Appl. 4, No. 2, 133-138.

[47] Hager,I., Rammah, Y., Othman, H., Ibrahim, E., Hassan, S., Sallam, F. (2019). Nano-structured natural bentonite clay coated by polyvinyl alcohol polymer for gamma rays attenuation, Journal of Theoretical and Applied Physics., 13, 141–153.

[48] Zughbi, A., Kharita, M.H., Shehada, A.M. (2017). Determining optical and radiation characteristics of cathode ray tubes' glass to be reused as radiation shielding glass. Radiation Physics and Chemistry, 136, 71–74.

[49] Ce, A., Champagnon, B., Martinez, V., Maksimov, L., Yanush, O., Bogdanov, V.N., 2006. xPbO–(1−x)GeO2 glasses as potential materials for Raman amplification. Opt. Mater. 28, 1301–1304. http://dx.doi.org/10.1016/j.optmat.2006.02.016.

[50] Othman, H.A., Elkholy, H.S., Hager, I.Z., 2016. FTIR of binary lead borate glass: structural investigation. J. Mol. Struct. 1106, 286–290. http://dx.doi.org/10.1016/j.molstruc. 2015.10.076.

[51] Hafiz, M. S., Othman, H.A., Kawady, N. A., Hager,I. Z., El-Feky, M. G., El-Samman, H. M. (2021). Structural Properties and Gamma Rays Shielding of TeO2-B2O3-PbO Glass System. J. Rad. Nucl. Appl. 6, No. 1, 31-38.

[52] Aloraini, Dalal Abdullah, Sayyed, M.I., Almuqrin, Aljawhara A.H., Kumar, Ashok, Khazaalah, Thair Hussein, Yasmin, Sabina, Khandaker, Mayeen Uddin, Baki, S.O. (2022). Preparation, radiation shielding and mechanical characterization of PbO–TeO2–MgO–Na2O–B2O3 glasses. Radiation Physics and Chemistry, 198, 110254.